DISCRETE RESONANCES

FRANCO VIVALDI

ABSTRACT. The concept of resonance has been instrumental to the study of Hamiltonian systems with divided phase space. One can also define such systems over discrete spaces, which have a finite or countable number of points, but in this new setting the notion of resonance must be re-considered from scratch. I review some recent developments in the area of arithmetic dynamics which outline some salient features of linear and nonlinear stable (elliptic) orbits over a discrete space, and also underline the difficulties that emerge in their analysis.

Dedicated to Professor Hao Bailin, on the occasion of his 80th birthday.

1. INTRODUCTION

In the early developments of modern dynamics, the pioneering work of B. V. Chirikov achieved a description of generic Hamiltonian systems —neither integrable nor ergodic— in terms of interactions between nonlinear resonances [8]. The prototype model of a nonlinear resonance is the set of librations of a pendulum. In appropriate units, Newton's equation of motion reads $\ddot{x} = -\sin(x)$, where x is the angular displacement from the stable equilibrium. Rewriting this differential equation in Hamilton's form

$$(\dot{x},\dot{y}) = (y, -\sin(x)), \tag{1}$$

we obtain a smooth vector field on an infinite cylinder. The energy $H(x,y) = y^2/2 - \cos(x)$ attains a minimum at the stable equilibrium: $H(0,0) = -1$. As the amplitude of the oscillations increases, their frequency decreases monotonically, reaching zero at the separatrices $H(x,y) = 1$. A nonlinear resonance is the domain bounded by the separatrices: $\{(x,y) : H(x,y) < 1\}$ (see figure 1).

We want to construct discrete versions of systems such as (1), and the first stage of this process consists of discretising time. There are various ways of doing this. One option is to consider the time-advance map $(x(t),y(t)) \mapsto (x(t+h),y(t+h))$, which is area-preserving for all h, since the vector field (1) has zero divergence. However, transforming a flow into a map in this way does not produce new dynamics.

Far more interesting is the time-discretisation associated with numerical integration algorithms, which introduces a perturbation of the original system. For our purpose it suffices to consider Euler's method, a basic numerical integration scheme which performs an approximate time-h advance map of the solutions of (1), with an error of order $O(h^2)$. Euler's method can be made area-preserving (i.e., symplectic) by adding a correction of order h^2:

$$\begin{aligned} x_{k+1} &= x_k + h\,y_k - h^2\sin(x_k) = x_k + h\,y_{k+1} \\ y_{k+1} &= y_k - h\sin(x_k). \end{aligned} \tag{2}$$

One verifies that the Jacobian matrix of this map has unit determinant.

Date: November 23, 2015.

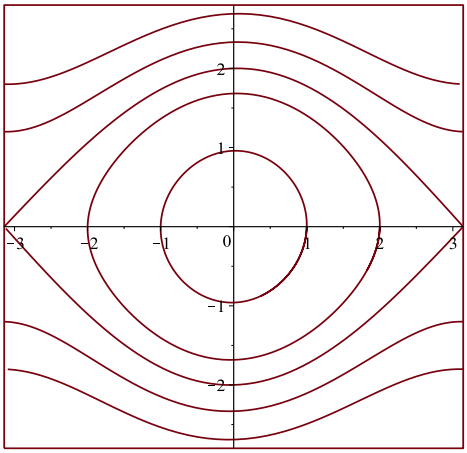

Figure 1: Orbits of the pendulum Hamiltonian, with a nonlinear resonance.

To bring the effect of time-discretisation to the foreground, we push the time-step h beyond a legitimate range, choosing $h = 0.9$, say (figure 2). The phase portrait now shows familiar features of near-integrable symplectic maps. This is no coincidence: the mapping (2) is conjugate to the celebrated Chirikov-Taylor's standard mapping [27, section 3.1]

$$\begin{aligned} p_{t+1} &= p_t + \varepsilon \sin(q_t) \\ q_{t+1} &= q_t + p_{t+1} \end{aligned} \tag{3}$$

via the coordinate change $q = -x$, $p = hy$, together with the reparametrization $\varepsilon = h^2$. (This conjugacy breaks down at $h = 0$, where Euler's map reduces to the identity, while the standard map is a shear.)

The mapping (2) commutes with translations by $2\pi/h$ in the y-direction, which makes the phase portrait doubly periodic. As a result, in addition to the original fixed points of the system (1) —the stable and unstable equilibria of the pendulum— an infinite sequence of spurious fixed points appears, in correspondence of the values of y for which the frequency of rotation of the pendulum is an integer multiple of the integration step. This gives rise to an infinite sequence of nonlinear resonances, evenly spaced along the cylinder at position $y = 2n\pi/h$, $n \in \mathbb{Z}$.

For small h, these resonances lie far apart from each other. Their mutual interaction is very small, but it does produces a dense set of secondary resonances, whose frequencies are rational multiples of the integration step. The new resonances appear near to every point in phase space, creating island chains and stochastic layers, which alter dramatically the small-scale structure of regular orbits. Increasing the time-step h has the effect of bringing the primary resonances closer together, and for sufficiently large h, exponential instability develops on a large scale. Chirikov characterised the critical h-value in terms of the overlap of the primary resonances.

While we recognise that time discretisation may give rise to new and interesting dynamics, our job is still incomplete. We must now embark in a second —and more difficult— discretisation process: discretizing space. This process will bring us closer to computer representations of dynamical systems.

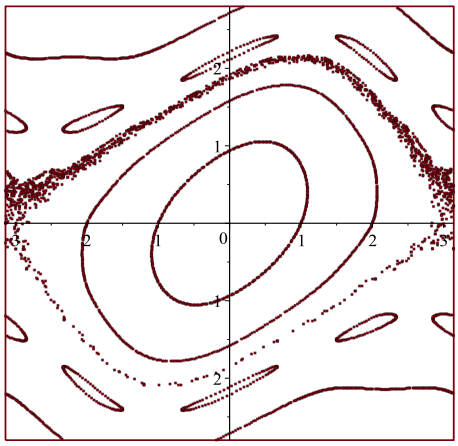

Figure 2: Phase portrait of the area-preserving map (2), with $h = 0.9$, showing a mixture of regular orbits, island chains, and chaotic orbits.

The study of Hamiltonian systems with discrete phase space has attracted the attention of researchers for many years. These works however, do not form a coherent body of research, let alone a proper mathematical theory. Following the pioneering work of Rannou [36], space discretisation has been considered for the most varied reasons: to achieve invertibility in a delicate numerical experiment [21], to mimic quantum effects in classical systems [15], to characterize periodic orbits in chaotic systems arithmetically [35, 9, 17, 32], to explore the structure of numerical orbits [22, 42, 18, 45, 28, 33].

In all Hamiltonian systems mentioned above, space discretisation is performed in such a way as to preserve invertibility. If this is achieved by merely restricting an invertible system to a discrete set, then no spurious perturbation accompanies space discretisation. For example, for algebraic symplectic maps with rational coefficients, the co-ordinates may be restricted to rational or algebraic numbers. (Most of the research in this area is devoted to dissipative systems, and we shall not deal with it for reasons of space. For background reference, see [43].) More often however, the space is discretised by a truncation process, which acts as a small perturbation of the original system; in the invertible case, such a perturbation will generate fluctuations without dissipation.

On a finite phase space all orbits are periodic; otherwise some orbits may escape to infinity in both time directions. The problem of stability under space discretisation now takes centre stage, particularly if the continuum system is stable, as it is in a resonance. The main difficulty originates from the fact that, in the limit of vanishing discretisation length, round-off perturbations are not smooth. So, even though these perturbations are still canonical, standard perturbation methods are not applicable.

We remark that the aforementioned scenario is not relevant to computations with floating-point arithmetic, which is the norm in numerical experiments. The floating-point numbers form a peculiar subset of the rationals, exponentially clustered about the origin, and this distribution is incompatible with the invariant uniform distribution (Lebesgue measure) of a symplectic map. This discrepancy results in large-scale irreversibility: all discrete orbits eventually reach a small invariant subset of

the set of floating-point numbers, which features an approximate uniform distribution [18] (see also [10, 6, 48, 23]).

Before attempting to construct a mathematical theory of such a complex dynamics, there are simpler problems to be considered. The first problem is uniform space discretisation of linear planar rotations —the time-advance maps of the harmonic oscillator. We force the system onto a lattice by a round-off procedure, and since the continuum dynamics is regular and well-understood, the effect of discretisation can be isolated from other dynamical phenomena. This problem, which has attracted considerable attention, is far from trivial [6, 45, 7, 48, 23, 28, 29, 30, 13, 12, 47, 26, 37, 38].

An alternative approach is to consider an affine twist map of a discrete space, and then add to it a suitable (piecewise) affine perturbation, which leaves such a space invariant without resorting to round-off. For example, the standard map (3) with $\varepsilon = 0$ leaves all rational lattices on the two-dimensional torus invariant. One must then choose functions $\varepsilon f(q)$ which preserve such lattices. This approach, which has been much exploited for maps of the continuum, has received remarkably little attention in the discrete case [50].

A third method for space discretisation is based on repeated applications of a simple scattering mechanism, which appears in outer billiards of convex polygons and their generalisations [40, 39, 38]. We consider a bundle of parallel rays which cross a line l on the plane, and which are refracted by it while remaining parallel (figure 3, left). The dynamics along rays is generated by a piecewise-constant velocity field $\mathbf{v}$ which assumes the values $\mathbf{v}_1$ and $\mathbf{v}_2$ on the two half-planes determined by l. The orbits of the flow $\dot{z} = \mathbf{v}(z)$ are parallel rays joined at l.

Next we perturb the flow by turning it into a map:

$$F_\lambda : \mathbb{R}^2 \to \mathbb{R}^2 \qquad F_\lambda(z) = z + \lambda \mathbf{v}(z), \tag{4}$$

where $\lambda > 0$ is the perturbation parameter. The map F_λ agrees with the time-λ advance map of the flow, except in the strip Σ bounded by the lines l and $F_\lambda^{-1}(l)$. Upon crossing the line l, an orbit of

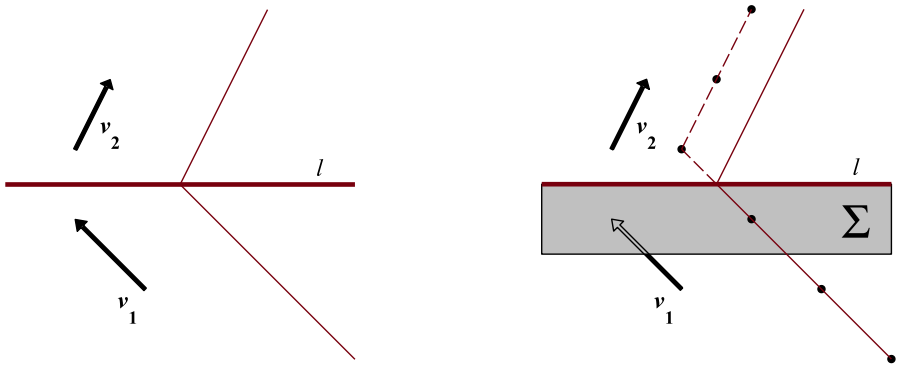

Figure 3: Rays scattered by a surface l. Left: the unperturbed flow. Right: a perturbed orbit of the map F_λ in (4) (black dots), which departs from the unperturbed orbit after crossing the strip Σ (dashed line).

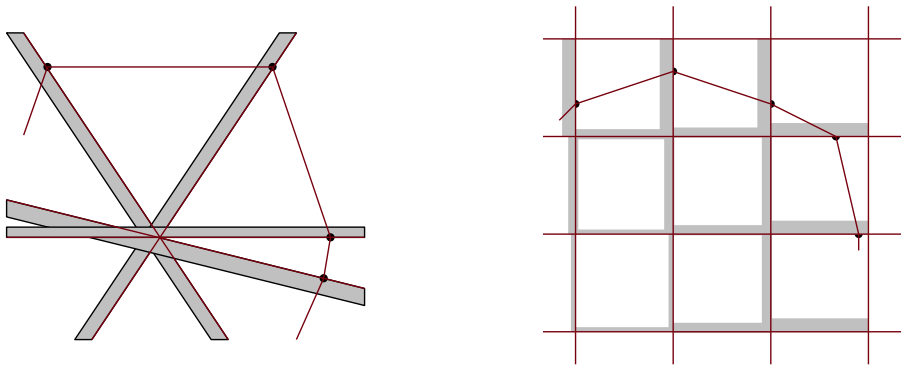

Figure 4: Schematic representation of the linked strip map construction, where the size of the perturbation is determined by the width of the strips. Left: outer billiard of a polygon. Right: the near rational discretised rotations described in section 5.

F_λ will jump from an orbit of the flow to a nearby orbit, which we interpret as a perturbation of the original motion (figure 3, right). The map F_λ is area-preserving, and if the orthogonal components of the incoming and outgoing fields are the same, then F_λ is invertible. Furthermore, any lattice generated by $\mathbf{v}_1$ and $\mathbf{v}_2$ will be F_λ-invariant, and hence this construction leads naturally to dynamics on lattices.

By varying the parameter λ, we can adjust the width of Σ, hence the size of the perturbation. With a suitable arrangement of scattering lines and fields, it is then possible to construct an interesting class of dynamical systems on lattices, which are perturbations of flows on polygons, and of which the outer billiards are the best known examples (figure 4). These dynamical systems will be called *linked strip maps*.

The purpose of this paper is to survey works on regular motions (rotations) in two-dimensional discrete spaces [45, 28, 29, 50, 30, 13, 12, 47, 26, 37, 38], underlying the mathematical tools needed for their analysis. These spaces will be embedded in smooth manifolds, and since this can be done in many ways, the choice of the manifold will be decisive. In section 2 we introduce a spatial discretisation of a family of linear elliptic maps, which results in weakly nonlinear systems on lattices. The analysis splits into three cases. *i*) Rational rotations (section 3), where the embedding space is the two-torus, and the dynamics is a piecewise isometry (zero entropy). *ii*) Irrational rotations (section 4), where the embedding space is the ring of p-adic integers and the dynamics is Bernoulli (positive entropy). *iii*) A near-rational case (section 5), where the embedding space is the plane, and the dynamics is given by linked strip maps. Finally, in section 6 we describe a parametrised family of perturbed twist maps on a lattice, whose Poincaré map is an interval-exchange transformation of the integers, with infinitely many intervals.

All dynamical systems mentioned above are found to be globally stable, even though this result has been established only in few cases. Typically, on a discrete space there are no invariant ‘circles’

to confine orbits, standard Hamiltonian perturbation methods do not apply, and the mechanisms that induce stability in such systems seem to be as varied as the systems themselves.

2. A MODEL FOR DISCRETE ELLIPTIC MOTIONS

A prototype for discrete linear elliptic motions is the lattice map

$$\Phi : \mathbb{Z}^2 \mapsto \mathbb{Z}^2 \qquad (x,y) \mapsto (\lfloor \lambda x \rfloor - y, x) \qquad \lambda = 2\cos(2\pi\nu) \tag{5}$$

where $\lfloor \cdot \rfloor$ is the floor function, the largest integer not exceeding its argument [45, 28, 29, 30, 13, 12, 47, 26].

One verifies that Φ is invertible. Without the floor function, equation (5) represents a one-parameter family of linear maps of the plane, conjugate to rotation by the angle $2\pi\nu$. These maps are represented by the family of matrices

$$C = \begin{pmatrix} \lambda & -1 \\ 1 & 0 \end{pmatrix} \qquad |\lambda| < 2 \tag{6}$$

and we shall use the same symbol C for both the matrix and the planar map represented by it. The floor function models the effect of round-off, pushing the point $(\lambda x - y, x)$ to the nearest lattice point on the left. This procedure is arithmetically nicer than the more orthodox rounding to the nearest lattice point, and it still produces a similarly rich dynamics. The lattice map should be regarded as a discrete approximation of the planar map: the discretisation length is fixed, and the limit of vanishing discretisation corresponds to motions at infinity.

The following unsolved question [1, 46] distils the difficulties encountered in the analysis of this model.[1]

Conjecture 1. *For all real λ with $|\lambda| < 2$, all orbits of Φ are periodic.*

Due to invertibility, periodicity is equivalent to boundedness. This conjecture holds trivially for $\lambda = 0, \pm 1$, the parameter values for which the map Φ is of finite order. Beyond this, the boundedness of all round-off orbits has been proved for only *eight* values of λ —see section 3.

The parameter of the map (5) may be chosen to be either the trace λ or the rotation number ν. Apart from trivial exceptions, a rational value of λ corresponds to an irrational value of ν, and vice-versa [31, chapter 2]. We shall consider three natural spaces in which to embed the lattice $\mathbb{Z}^2$, corresponding, respectively, to rational values of ν, rational values of λ, and a particular range of near-integer values of λ. The resulting dynamics are very different in these cases, and so are the mathematical tools needed to study them.

3. RATIONAL ROTATIONS AND PIECEWISE ISOMETRIES

If in equation (5) we let $\nu = p/q$, a rational number, then the qth iterate of the matrix (6) —the linear map without round-off— is the identity. The qth iterate of the map (5) will then be 'close to the identity', and it makes sense to consider the discrete vector field

$$\mathbf{v}(z) = \Phi^q(z) - z \qquad z = (x,y) \in \mathbb{Z}^2 \tag{7}$$

which can be shown to be uniformly bounded, that is, to assume only finitely many values. This construction may be seen as a discrete analogue of the vector field approximations of perturbed area-preserving diffeomorphisms at resonance [3, section 6.2.2.]. Some integral curves of this vector field are displayed in figure 5. It is plain that the effect of round-off cannot be described as the addition of deterministic noise to the system. The round-off perturbation rather generates a highly organised

[1] A related general conjecture on the boundedness of discretised invertible rotations was first formulated in [6].

(self-similar) fractal structure, which displays rotations about secondary centres —a skeletal form of 'island chains'.

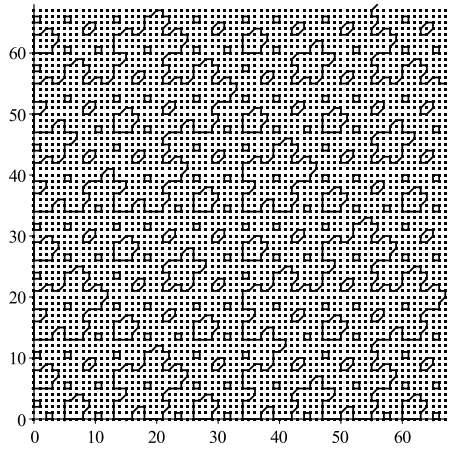

Figure 5: Integral curves of the discrete vector field (7) on the first quadrant of the lattice $\mathbb{Z}^2$, for the parameter $\nu = 1/5$. The dots represent fixed points of the map Φ^5. The other curves form polygons with an increasing number of sides —a sort of surrogate island chains— which suggest successive approximations to a fractal Koch snowflake.

Arithmetically, the resonant condition $\nu \in \mathbb{Q}$ implies that λ is an algebraic integer —a root of a monic polynomial with integer coefficients. The degree of such a polynomial is $\phi(q)/2$, where ϕ is Euler's function [24, section 5.5]. The simplest scenario occurs for $\phi(q) = 4$, corresponding to the following values of ν:

$$\nu = \frac{1}{5}, \frac{2}{5}, \frac{1}{8}, \frac{3}{8}, \frac{1}{10}, \frac{3}{10}, \frac{1}{12}, \frac{5}{12}. \tag{8}$$

(Figure 5 corresponds to the first entry in the list.) For these values, the minimal polynomial of λ is quadratic, and we shall denote by $\bar{\lambda}$ the algebraic conjugate of λ (the other root of the minimal polynomial of λ).

To study the lattice dynamics for these parameter values, we introduce the fundamental domain $\Omega = [0,1)^2$ of the torus $\mathbb{R}^2/\mathbb{Z}^2$, and consider the *torus map*

$$\bar{\Phi} : \Omega \to \Omega \qquad \zeta \mapsto (\bar{C} \cdot \zeta - \mathbb{Z}^2) \cap \Omega \tag{9}$$

where $\bar{C}$ is the algebraic conjugate matrix of the matrix C of (6). We have the following result [26, Theorem 1]:

Theorem 1. *For all values of ν listed in (8), the mapping Φ is dual to the mapping $\bar{\Phi}$, in the sense that there is a uniform embedding*

$$\mathscr{E} : \mathbb{Z}^2 \to \Omega \qquad (x,y) \mapsto (x - m_0/\lambda, y - m_1/\lambda)$$

where m_0 and m_1 are integers uniquely determined by the condition $\mathscr{E}(x,y) \in \Omega$.

The torus map (9) is linearly conjugate to a piecewise isometry. Namely, there is a finite partition $\Omega = \cup_i \Omega_i$ into convex polygons Ω_i such that over each Ω_i the map $\bar{\Phi}$ is the composition of a rotation and an i-dependent translation.

This representation allows one to prove the following result.

Theorem 2. *For all values of ν listed in (8), all orbits of the map Φ are periodic.*

The case $\nu = 1/5$, corresponding to $\lambda = (1-\sqrt{5})/2$ was established in [28], with computer assistance. Similar techniques were used to extend the result to the other parameter values in (8), for a set of initial conditions having full density [26]. An analytical proof of the conjecture for the eight parameters (8) and all initial conditions was eventually given in [2]. In all cases, periodicity was established using renormalisation techniques.

For any other rational value of ν, there is a similar embedding in piecewise isometries of a higher-dimensional tori [26]. These systems are still unexplored, even in the cubic case.

4. Irrational rotations and p-adic numbers

If the rotation number ν is irrational, then the orbits of the linear map C are dense on invariant ellipses. In this regime, the round-off perturbation introduces a form of small-amplitude deterministic randomness, as illustrated in figure 6. In all experiments performed to date, all orbits have been found to be periodic, arranged along the invariant curves of the integrable system. However, their period as a function of the distance from the origin (inverse discretisation length) shows very large fluctuations, which are the root cause of the difficulties in proving the periodicity conjecture.

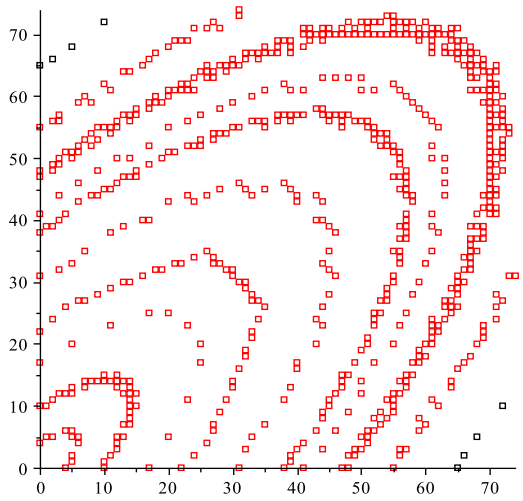

Figure 6: Orbits of the mapping Φ on the first quadrant of $\mathbb{Z}^2$. The parameter is $\lambda = 1/2$, corresponding to an irrational rotation number ν. All displayed orbits are periodic, and they are arranged along the invariant ellipses of the linear map C.

On first inspection, the origin of these fluctuations is unclear. One would expect some form of exponential instability, but the standard indicators of chaotic behaviour give negative reading here. Moreover, even for time intervals which are short compared to the orbital period, the distance between points of initially close orbits does not show any sign of exponential growth. Likewise, the number of periodic orbits with period less than T grows very slowly with T —certainly non exponentially.

It turns out that the round-off fluctuations are indeed the result of deterministic chaos, more precisely, they are a feature of periodic orbits of a smooth system with positive entropy. However, to see this it is necessary to look elsewhere, and embed the lattice $\mathbb{Z}^2$ in an appropriate space.

The essence of this phenomenon is already in full view for a special set of *rational* values of the parameter λ, namely

$$\lambda = \frac{q}{p^n} \qquad p \text{ prime} \qquad |q| < 2p^n. \tag{10}$$

Since λ is irrational but not an integer, it follows that the rotation number ν is irrational [31, chapter 2].

It turns out that for this choice of parameters the map Φ admits an embedding into an expanding map of the ring of p-adic integers $\mathbb{Z}_p$, and the mapping Φ^*, which is conjugate to Φ on the image of $\mathbb{Z}^2$ in $\mathbb{Z}_p$, is Bernoulli.

The new phase space $\mathbb{Z}_p$ consists of all expressions of the type

$$\chi = \sum_{k=m}^{\infty} c_k p^k \qquad c_k \in \{0,\dots,p-1\}, \quad m \geqslant 0, \quad c_m \neq 0 \tag{11}$$

which converge with respect to the p-adic absolute value

$$|\chi|_p = \frac{1}{p^m}. \tag{12}$$

The function $|\cdot|_p$ assumes discrete values, and it satisfies the ultrametric inequality

$$|\chi + \chi'|_p \leqslant \max(|\chi|_p, |\chi'|_p). \tag{13}$$

With the topology induced by $|\cdot|_p$, the set $\mathbb{Z}_p$ is a Cantor set. For background bibliography on p-adics, see [20]. Research is the area of p-adic dynamics is well-developed: see [5] for an accessible introduction, and [13, 12, 47, 34, 49] for some relevant literature.

When $\lambda = q/p^n$ in (5), there are p^n possible values for the round-off kick. Accordingly, we define a symbolic dynamics on p^n symbols as follows

$$c : \mathbb{Z}^2 \to \{0,\dots,p^n-1\} \qquad (x,y) \mapsto x \,(\mathrm{mod}\ p^n). \tag{14}$$

The next results were proved in [13]. The first one characterizes the cylinder sets of the symbolic dynamics, namely the set of lattice points whose symbol sequence begins with a specified code of length k, which we call a *k-code*.

Lemma 3. *There exists a nested sequence of lattices*

$$L_1 \supset L_2 \supset L_3 \supset \cdots$$

with $|\mathbb{Z}^2/L_k| = p^{nk}$, with the property that two points in $\mathbb{Z}^2$ have the same k-code if and only if they are congruent modulo L_k.

This peculiar notion of closeness —congruence modulo a lattice with a large fundamental domain— is the signature of a non-archimedean metric (12). Note that *all* finite codes of the symbolic dynamics (14) are represented by orbits in $\mathbb{Z}^2$. Furthermore, defining the density $D(X)$ of a set $X \subset \mathbb{Z}^2$ as

$$D(X) = \lim_{N\to\infty} \frac{1}{(2N)^2} \#\{(x,y) \in X : \max(|x|,|y|) < N\} \tag{15}$$

we see that any k-cylinder set in $\mathbb{Z}^2$ has density p^{-nk} in $\mathbb{Z}_p$.

To justify the appearance of the lattices L_k we consider the modular identity

$$f(x) = x^2 - qx + p^{2n} \equiv x(x-q) \,(\mathrm{mod}\ p). \tag{16}$$

The polynomial $f(x)$ is irreducible in $\mathbb{Q}$, having negative discriminant. Moreover, the factors of $f(x)$ modulo p are distinct, because p and q are co-prime. Let α be a root of $f(x)$ [thus α is a scaled eigenvalue of the matrix C in (6)], and let us consider the ring

$$\mathbb{Z}[\alpha] = \{m + n\alpha \,:\, m,n \in \mathbb{Z}\}.$$

The factorization (16) implies that the prime p splits in $\mathbb{Z}[\alpha]$ into the product of two distinct prime ideals: $p\mathbb{Z}[\alpha] = P\overline{P}$. Recall that an ideal in a ring is an additive group closed under multiplication by ring elements. Geometrically, these ideals are two-dimensional lattices, and the product $P\overline{P}$ alluded above is defined as the set of all finite sums $\pi_1\overline{\pi}_1 + \cdots + \pi_s\overline{\pi}_s$ with $\pi_i \in P$ and $\overline{\pi}_j \in \overline{P}$ [31, chapter 3].

The next result shows that the discrete phase space $\mathbb{Z}^2$, as well as its sub-lattices L_k, are in fact more than two-dimensional lattices.

Lemma 4. *The embedding*

$$\mathscr{L}_1 : \mathbb{Z}^2 \to \mathbb{Z}[\alpha] \qquad (x,y) \mapsto px - \alpha y$$

defines an isomorphism $\mathbb{Z}^2 \sim P^n$ of $\mathbb{Z}$-modules such that, for all $k \geqslant 1$, we have $L_k \sim P^{n(k+1)}$.

This result provides the discrete phase space $\mathbb{Z}^2$ of the round-off map Φ with a multiplicative structure, much like going from $\mathbb{R}^2$ to $\mathbb{C}$. Now, for all positive k, the finite ring $\mathbb{Z}[\alpha]/P^k$ is isomorphic to $\mathbb{Z}/p^k\mathbb{Z}$. Under this isomorphism, an element ζ in $\mathbb{Z}[\alpha]$ maps to a unique residue class modulo p^k, and the sequence of these residue classes converges to a p-adic number. In particular, the complex roots of $f(x)$ correspond to the roots of $f(x)$ in $\mathbb{Z}_p$. We denote the latter by φ and $\overline{\varphi}$; they are identified as follows (cf. (16)):

$$\varphi \equiv 0 \,(\mathrm{mod}\ p) \qquad \overline{\varphi} \equiv q \,(\mathrm{mod}\ p). \tag{17}$$

Because q is co-prime to p, we have that $|\overline{\varphi}|_p = 1$, that is, $\overline{\varphi}$ belongs to the p-adic unit circle (in arithmetical parlance, $\overline{\varphi}$ is a *p-adic unit*), while $|\varphi|_p < 1$. The computation of φ and $\overline{\varphi}$ is performed efficiently with the p-adic Newton's method, which is super-convergent [41, chapter 2]. From equations (17) we see that the initial condition for the Newton recursive sequence $\varphi_k \to \varphi$ is $\varphi_0 = 0$, whereas $\overline{\varphi}_0 = q$.

Identifying α with φ defines an embedding $\mathscr{L}_2$ of $\mathbb{Z}[\alpha]$ into the ring $\mathbb{Z}_p$ of p-adic integers:

$$\mathscr{L}_2 : \mathbb{Z}[\alpha] \to \mathbb{Z}_p \qquad x + \alpha y \mapsto x + \varphi y.$$

Composing $\mathscr{L}_1$ and $\mathscr{L}_2$ and scaling gives us the desired embedding.

Theorem 5. *The dense embedding*

$$\mathscr{L} : \mathbb{Z}^2 \mapsto \mathbb{Z}_p \qquad (x,y) \mapsto \frac{1}{p}\mathscr{L}_2(\mathscr{L}_1(x,y)) = x - \frac{\varphi}{p^n}y \tag{18}$$

has the property that the mapping $\Phi^* = \mathscr{L} \circ \Phi \circ \mathscr{L}^{-1}$ can be extended continuously from $\mathscr{L}(\mathbb{Z}^2)$ to the whole of $\mathbb{Z}_p$, giving

$$\chi_{t+1} = \Phi^*(\chi_t) = \sigma^n(\overline{\varphi}\,\chi_t) \tag{19}$$

where $\overline{\varphi} = \mathscr{L}(q, p^n)$ is a p-adic unit and σ is the shift mapping.

The shift σ is defined as its archimedean counterpart; if $\chi = c_0 + c_1 p + c_2 p^2 + \cdots$, then

$$\sigma(\chi) = c_1 + c_2 p + c_3 p^2 + \cdots . \tag{20}$$

The p-adic shift mapping has been studied in [44, 4, 49].

The above result represents the round-off problem on $\mathbb{Z}^2$ as a sub-system of an expanding map over the p-adics, which preserves the standard probability measure on $\mathbb{Z}_p$ (the additive Haar measure), obtained by assigning to each residue class modulo p^k the measure p^{-k}. This is just the natural measure on $\mathbb{Z}_p$ as a Cantor set.

The map Φ^* has a complete symbolic dynamics over p^n symbols, and a dense set of unstable periodic orbits. All t-cycles of Φ^* have multiplier p^{-nt}. It is possible to show that all periodic points are p-adic integers, and that their closure is the p-adic unit disc $\{\chi \in \mathbb{Z}_p : |\chi|_p \leq 1\}$. This system calls to mind the dynamical system given by multiplication by p^n on the circle: $x \mapsto p^n x \,(\mathrm{mod}\, 1)$ [25, section 1.7]. In both maps, the positive metric entropy of the embedding dynamical system provides an essential substrate for the existence of irregular motion on lattices. (See [19] for a friendly introduction to the question of algorithmic complexity in this shift system, and [16] for a parallel with quantum dynamics.)

The symbol sequences generated by the round-off orbits are good pseudo-random sequences (a comparison with [49] is instructive). Some rigorous results will be found in [47], most notably a central limit theorem governing the departure of round-off orbits from exact orbits. However, as is often the case in this type of problems, the most interesting phenomena are difficult to analyse. Experimentally, the period of the orbits is found to grow —on average— proportionally to the height of the initial condition (the 'seed' of the pseudo-random sequence), while displaying at the same time huge fluctuations. The latter suggest that the period function is hard to compute —a good candidate for a non-polynomial time problem. The symbol sequences corresponding to $\lambda = 1/2$ have been tested at Hewlett Packard [14]. They feature good pseudo-randomness for short times, and faint correlations at certain larger times, related to the denominators of good rational approximants of the rotation number.

5. Near-rational rotations and linked strip maps

The third regime of discretised rotations Φ to be considered is the limit $\lambda \to 0$, corresponding to $\nu \to 1/4$ in (5). The asymptotic dynamics provides an example of the linked strip maps construction discussed in the introduction. At $\lambda = 0$ the dynamics is trivial: there is no round-off and the mapping has order four. This time the natural embedding of $\mathbb{Z}^2$ is the plane $\mathbb{R}^2$, and the dynamics for $\lambda \to 0$ is best described as a perturbation of a weakly nonlinear piecewise-smooth integrable Hamiltonian system [see (24) below]. For this reason, this limit will be referred to as the *integrable limit* [37, 38].

As λ approaches 0, the iterated map F^4 is close to the identity, suggesting the introduction of a *discrete vector field* on the scaled lattice $(\lambda\mathbb{Z})^2$:

$$\mathbf{v}_\lambda(z) = F_\lambda^4(z) - z, \qquad F_\lambda(z) = \lambda F(z/\lambda) \qquad \lambda > 0 \tag{21}$$

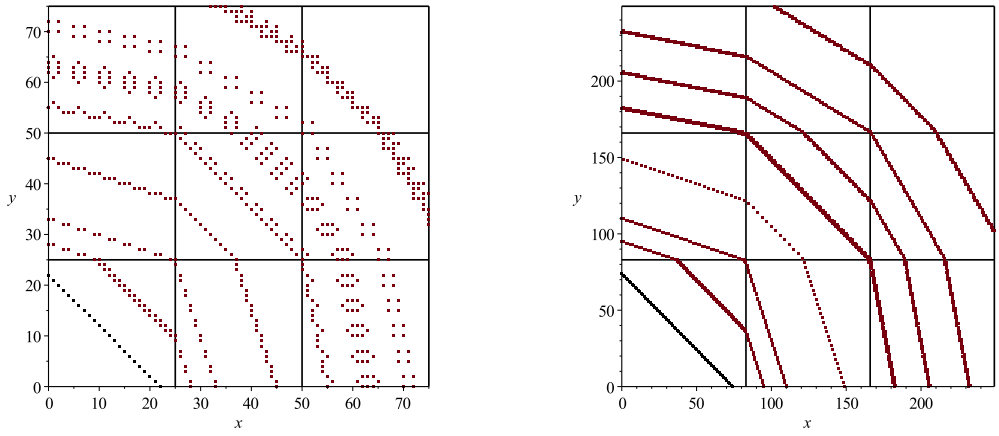

Figure 7: Some periodic orbits of the rescaled map F_λ for $\lambda = 1/25$ (left) and $\lambda = 1/83$ (right). The view is restricted to the first quadrant. The discrete island chains visible on the left are not visible on the right due to their small size. It is apparent that some scaling is necessary for convergence to an integrable system.

where $F_\lambda : (\lambda\mathbb{Z})^2 \to (\lambda\mathbb{Z})^2$ is a scaled version of (5). Unlike in (7), the field $\mathbf{v}_\lambda$ is not bounded; as $\lambda \to 0$, this field becomes piecewise-constant, albeit in a non-uniform manner. The domains over which the vector field is constant converge to squares, bounded by an infinite array of orthogonal lines (figure 7). The phase portrait suggests a coarse version of divided phase space, with small-scale features receding to the background as $\lambda \to 0$.

More precisely, over any bounded domain of the plane, the integrable Hamiltonian vector field $\mathbf{w}$

$$\mathbf{w} : \mathbb{R}^2 \to \mathbb{Z}^2 \qquad \mathbf{w}(x,y) = (2\lfloor y \rfloor + 1, -(2\lfloor x \rfloor + 1)). \tag{22}$$

is such that $\lambda\mathbf{w}$ agrees with $\mathbf{v}_\lambda$ for all sufficiently small λ, apart from regions of vanishing total measure.

The domains of constant $\mathbf{w}$ are translated unit squares (called *boxes*)

$$B_{m,n} = (m,n) + [0,1)^2 \qquad m,n \in \mathbb{Z} \tag{23}$$

and the field across adjacent boxes is transversal. The corresponding Hamiltonian $\mathscr{H}$ is given by

$$\mathscr{H} : \mathbb{R}^2 \to \mathbb{R} \qquad \mathscr{H}(x,y) = P(x) + P(y), \tag{24}$$

where P is the piecewise-affine function

$$P : \mathbb{R} \to \mathbb{R} \qquad P(x) = \lfloor x \rfloor^2 + (2\lfloor x \rfloor + 1)\{x\}, \tag{25}$$

and $\{x\}$ denotes the fractional part of x. The level sets of the Hamiltonian $\mathscr{H}$ are convex polygons, with an increasing number of sides: near the origin they are squares, while at infinity they approach circles. For small λ, the fourth iterate of F_λ is equal to the time-λ advance map of the flow along

the edges of the polygons. The perturbation occurs near the vertices, where the orbits of $\mathscr{H}$ are not differentiable.

Thus, in the integrable limit, the rescaled map F_λ is a perturbation of an integrable Hamiltonian system, but the integrable system is no longer a rotation, and the perturbation is no longer caused by round-off. The perturbation mechanism is of the *linked strip maps* type (see figure 4, right), which resembles the 'pinwheel map' introduced by Schwartz as a generalisation of outer billiards of convex polygons [40, 39] (figure 4, left). Note that as the distance from the origin increases, the number of strips encountered by individual orbits increases without bounds. As a result, the integrable system is nonlinear, i.e., its time-advance map satisfies a twist condition.

More precisely, the level curves of $\mathscr{H}$ passing through integer points $(m,n) \in \mathbb{Z}^2$ subdivide the plane into annular regions called *polygon classes*, with all polygons in a class having the same number of vertices. Each polygon class is indexed by the value $e \in \mathscr{E}$ of $\mathscr{H}$ at its inner boundary, where $\mathscr{E}$ is the set of integers representable as the sum of two squares (see [24, chapter XX]). Along the main diagonal (the symmetry axis of F_λ) we identify a rectangular strip X_e contained within the class, and whose width is equal to the magnitude of the vector field (figure 8). The strip X_e is crossed repeatedly by all orbits in that region, and serves as Poincaré surface of section for F_λ. Topologically, the set X_e is a cylinder, since opposite sides are identified via the action of F_λ.

As $\lambda \to 0$, the width of the strip X_e also goes to zero. By mapping the strip X_e to the infinite cylinder $\mathbb{S}^1 \times \mathbb{R}$, we obtain the following characterisation of the unperturbed Poincaré return map of each polygon class [38].

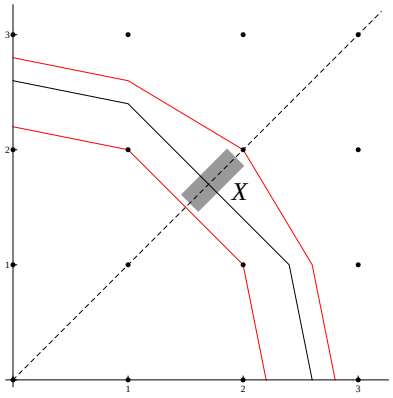

Figure 8: Surface of section for a polygon class.

Theorem 6. *Associated with each polygon class, indexed by $e \in \mathscr{E}$, there is a change of coordinates which conjugates the unperturbed return map to X_e to the linear twist map T^e, given by*

$$T^e : \mathbb{X} \to \mathbb{X} \qquad T^e(\theta,\rho) = (\theta + \kappa\rho, \rho)\,, \tag{26}$$

where $\mathbb{X}$ is the unit cylinder:

$$\mathbb{X} = \mathbb{S}^1 \times \mathbb{R},$$

and $\kappa = \kappa(e)$ is the twist. Furthermore, as $e \to \infty$, the limiting behaviour of $\kappa(e)$ is singular:

$$\kappa(e) \to \begin{cases} 4 & \{\sqrt{e}\} = 0 \\ 0 & \text{otherwise.} \end{cases}$$

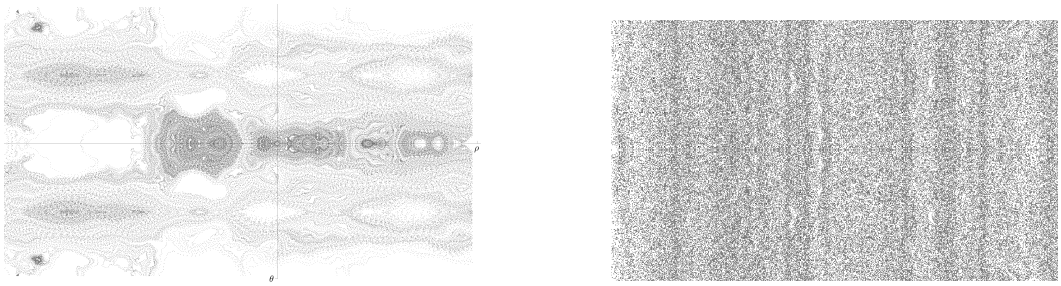

Figure 9: Orbits of the surface of section map on X_e in the cylindrical co-ordinates (θ,ρ) of equation (26). The width of the cylinder consists of approximately 500 lattice sites. Left: Resonances for $e = 160234 \approx 400.3^2$ and $\lambda \approx 3.5\times 10^{-9}$. Right: Pseudo-chaos for $e = 200^2$.

For any non-zero λ, the first-return map to the strip X_e is a perturbed twist map on a lattice. The twist condition is given by the theorem above, and the perturbation results from the cumulative effect of a large number of linked strip maps. We distinguish two regimes. For a polygon class where the twist $\kappa(e)$ tends to zero, the low nonlinearity amplifies the effect of the perturbation. As a result, a distinctive version of near-integrable Hamiltonian dynamics emerges on the lattice, featuring delicate resonance-like structures, superimposed to low-amplitude fluctuations (figure 9).

By contrast, at parameters where the twist persists (e is a large square), the arabesques disappear, and the featureless phase portrait suggests a form of 'pseudo-chaotic' dynamics. This type of dynamics has been observed in piecewise affine maps on lattices [32].

6. Discrete twist maps and interval-exchange transformations

We conclude our excursion into discrete rotational motions with a brief survey of a perturbed twist map on a lattice, defined as

$$\begin{aligned} y_{t+1} &\equiv y_t + f(x_t) \,(\mathrm{mod}\, N) \\ x_{t+1} &\equiv x_t + y_{t+1} \,(\mathrm{mod}\, N) \end{aligned} \tag{27}$$

where N is a large fixed integer (the discretisation parameter) and $f:\mathbb{Z}\to\mathbb{Z}$ is an N-periodic function. The phase space is a doubly-periodic lattice with N^2 points.

To turn (27) into a discrete version of the standard mapping (3) one would choose, say, $f(x) = \lfloor N\varepsilon \sin(x/N)\rfloor$, but this system is not amenable to a detailed analysis. A simpler choice for f was considered in [50]:

$$f(q) = \begin{cases} 1 & 0 \leqslant q < \lfloor N/2\rfloor \\ -1 & \text{otherwise.} \end{cases} \tag{28}$$

This map is invertible, and hence all its orbits are periodic. It features a discrete version of dynamics on a divided phase space, with a rudimentary form of island chains (figure 10).

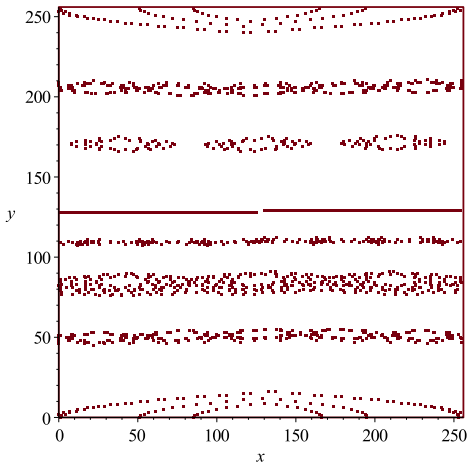

Figure 10: Orbits of the invertible mapping (27), for $N = 256$ and f given by (28).

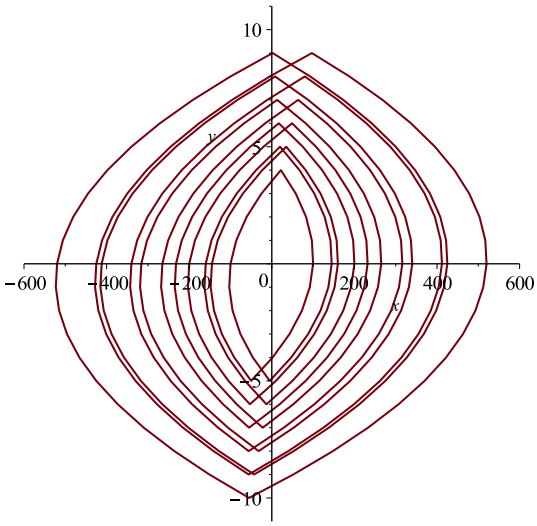

Figure 11: An orbit of the local map (29) for the parameters $\alpha = 11$, $\beta = 3$ and initial condition $(200, 0)$. The orbit performs complex radial excursions.

We are interested in the motion in such resonant regions. After changing to local co-ordinates centred at an elliptic fixed point, one finds that as $N \to \infty$, the dynamics of an island is described by the following lattice map of the plane [50, eq. (7)]:

$$\mathscr{F} : \mathbb{Z}^2 \to \mathbb{Z}^2 \qquad \begin{aligned} y_{t+1} &= y_t - \operatorname{sign}(x_t) \\ x_{t+1} &= x_t + \alpha y_{t+1} + \beta \end{aligned} \qquad 0 \leqslant \beta < \alpha \tag{29}$$

where α and β are integers determined by the rotation number of the island, and

$$\mathrm{sign}(x) = \begin{cases} 1 & \text{if } x \geqslant 0 \\ -1 & \text{if } x < 0. \end{cases}$$

In spite of a simple appearance, the map (29) has a non-trivial dynamics which is not well-understood (for a pseudo-hyperbolic variant of this model, see [32]).

It is not difficult to show that all orbits must intersect repeatedly the non-negative integer lattice $\mathbb{Z}_+$, as illustrated in figure 11. Thus we define a Poincaré first-return map F of this domain. Letting $\mathbb{Z}_-$ be the set of negative integers, we find that $F = F_- \circ F_+$ is the composition of the first transit maps $F_\pm$ from $\mathbb{Z}_\pm$ to $\mathbb{Z}$ induced by $\mathscr{F}$

$$F_+ : \mathbb{Z}_+ \to \mathbb{Z}, \qquad F_- : \mathbb{Z}_- \to \mathbb{Z}.$$

(Strictly speaking, this statement holds only at sufficient distance from the origin.)

The following conjecture (see [50]) captures a salient feature of the map (29).

Conjecture 2. *If α is not divisible by 4, then all orbits of F are periodic with period not exceeding $T = \alpha/\gcd(\alpha, 2\beta)$. Moreover, for all sufficiently large initial conditions, the period is exactly T.*

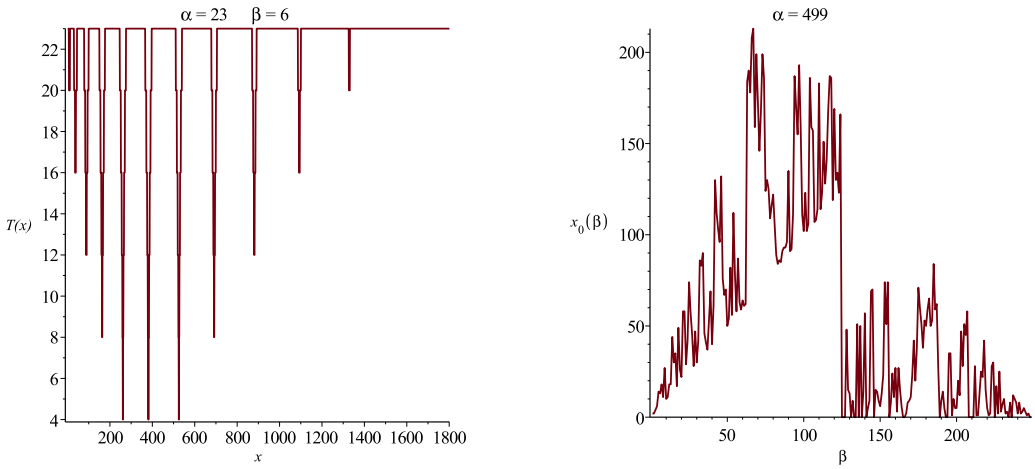

Figure 12: Left: Period $T(x)$ of the orbit of the Poincaré recurrence map F of equation (32) through the point x, for parameter values $\alpha = 23$, $\beta = 6$. The period eventually attains the value $\alpha/\gcd(\alpha, 2\beta) = 23$, according to conjecture 2. Right: the smallest integer $x_0 = x_0(\beta)$ such that $T(x_0) = \alpha$, for $\alpha = 499$ and $1 \leqslant \beta < \alpha/2$.

Let us investigate the map F more closely. To find an expression for $F_\pm$ we solve (29) over each domain where $\mathrm{sign}(x)$ is constant, and then match the solutions at the boundary line $x = 0$. We obtain

$$\begin{array}{rcll} F_+(x) & = & x + \tau_+(x) & x \geqslant 0 \\ F_-(x) & = & x + \tau_-(x) & x < 0 \end{array} \tag{30}$$

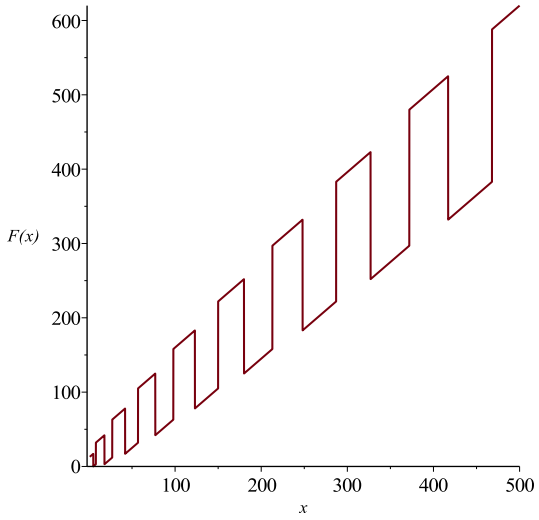

Figure 13: The interval-exchange map F of equation (32), for parameters $\alpha = 11$, $\beta = 3$.

where

$$
\begin{aligned}
\tau_+(x) &= 2\beta u_+(x) - \alpha u_+(x)^2 \\
u_+(x) &= \lfloor U_+(x) + 1 \rfloor \\
U_+(x) &= \frac{1}{2\alpha}\left(2\beta - \alpha + \sqrt{(2\beta-\alpha)^2 + 8\alpha x}\right) \\
\\
\tau_-(x) &= 2\beta u_-(x) + \alpha u_-(x)^2 \\
u_-(x) &= \lceil U_-(x) \rceil \\
U_-(x) &= \frac{1}{2\alpha}\left(-(2\beta+\alpha) + \sqrt{(2\beta+\alpha)^2 - 8\alpha x}\right).
\end{aligned}
\tag{31}
$$

The functions $\tau_\pm$ are singular, due to the presence of the floor and ceiling in $u_\pm$. Each function has an infinite sequence of singularities and is right-continuous at each singularity. The singularities have the density of the squares.

The above expressions enable us to write the first-return map F to $\mathbb{Z}_+$ explicitly:

$$
\begin{aligned}
F(x) &= F_-(F_+(x)) = x + \tau(x) \\
\tau(x) &= 2\beta(u_+(x) + u_-(y)) + \alpha(u_-^2(y) - u_+^2(x)) \qquad y = F_+(x).
\end{aligned}
\tag{32}
$$

The map F is invertible, and locally it reduces to a translation, being a composition of two translations. Hence F is an interval-exchange transformation. The singularities of F determine the end-points of the intervals being exchanged. and since there are infinitely many such singularities, we have an interval-exchange transformation with infinitely many intervals (figure 13). For all odd values of the parameter α, the interval-exchange dynamics causes all orbits of F to be be intertwined, i.e., there are no bounding invariant sets. According to conjecture 2, the period $T(x)$ of the orbits of F becomes

eventually constant for large x. However, near the origin such a period shows a non-trivial dependence on initial conditions as well as parameters (figure 12). In particular, the parameter dependence features large fluctuations of arithmetical origin.

REFERENCES

[1] S. Akiyama and H. Brunotte and A. Pethő and J. M. Thuswaldner, Generalized radix representations and dynamical systems II, *Acta Arith.* **121** (2006) 21–61.

[2] S. Akiyama and H. Brunotte and A. Pethő and W. Steiner, Periodicity of certain piecewise affine integer sequences, *Tsukuba J. Math.* **32** (2008) 197–251.

[3] D. K. Arrowsmith and C. M. Place *An introduction to dynamical systems*, Cambridge University Press, Cambridge (1990).

[4] D. K. Arrowsmith and F. Vivaldi, Some p-adic representations of the Smale horseshoe, *Phys. Lett. A*, **176** (1993) 292–294

[5] D. K. Arrowsmith and F. Vivaldi, Geometry of p-adic Siegel discs, *Physica D* **71** (1994) 222–236.

[6] M. Blank, Pathologies generated by round-off in dynamical systems *Physica D* **78** (1994) 93–114.

[7] M. Blank, *Discreteness and continuity in problems of chaotic dynamics*, volume 161 of *Translations of Mathematical Monographs*, American Mathematical Society, Providence, RI, USA (1997).

[8] B. V. Chirikov, A universal instability of many-dimensional oscillator systems, *Physics Reports*, **52** (1979) 263–379.

[9] M. Bartuccelli and F. Vivaldi, Ideal orbits of toral automorphisms, *Physica D* **39** (1989) 194–204.

[10] C. Beck and G. Roepstorff, Effects of phase space discretization on the long-time behavior of dynamical systems, *Physica D* **25** (1987) 173–180.

[11] N. Bird and F. Vivaldi, Periodic orbits of the sawtooth maps, *Physica* **30***D* (1988) 164–176.

[12] D. Bosio, Round-off errors and p-adic numbers, Queen Mary, University of London (2000).

[13] D. Bosio and F. Vivaldi, Round-off errors and p-adic numbers, *Nonlinearity* **13** (2000) 309–322.

[14] J. Castejon, private communication (2001).

[15] B. V. Chirikov, F. M. Izrailev, and D. L. Shepelyansky, Dynamical stochasticity in classical and quantum mechanics, *Soviet Scientific Reviews C, Vol.2*, Gordon and Breach, New York (1981) 209–267.

[16] B.V. Chirikov and F.Vivaldi, An algorithmic view of pseudochaos, *Physica D* **129** (1999) 223–235.

[17] M. Degli Esposti and S. Isola, Distribution of closed orbits for linear automorphisms of tori, *Nonlinearity* **8** (1995) 827–842.

[18] D. J. D. Earn and S. Tremaine, Exact numerical studies of hamiltonian maps: iterating without roundoff errors, *Physica D* **56** (1992) 1–22.

[19] J. Ford, How random is a coin toss?, *Physics Today* **36** (1983) 40–47.

[20] F. Q. Gouvêa, *p-adic numbers: An introduction*, Springer-Verlag, Berlin, second edition (1997).

[21] C. F. F. Karney, Long time correlations in the stochastic regime, *Physica D* **8** (1983) 360–380.

[22] K. Kaneko, Symplectic cellular automata, *Phys. Lett. A* **129** (1988) 9–16.

[23] V. Kozyakin, On finiteness of trajectories for one mapping associated with quasi-inversion of rotation mapping on integer planar lattice, preprint, Institute of Information Transmission Problems, Russian Academy of Sciences, Moscow (1997). [kozyakin@ippi.ac.msk.su]

[24] G. H. Hardy and E. M. Wright, *An introduction to the theory of numbers,* Oxford University Press, Oxford (1979).

[25] A. Katok and B. Hasselblatt, *Introduction to the Modern Theory of Dynamical Systems*, Cambridge University Press, Cambridge (1995).

[26] K. L. Kouptsov and J. H. Lowenstein and F. Vivaldi, Quadratic rational rotations of the torus and dual lattice maps, *Nonlinearity*, **15**, (2002) 1795–1482.

[27] A. J. Lichtenberg and M. A. Lieberman, *Regular and Stochastic Motion*, Springer-Verlag, New York (1983).

[28] J. H. Lowenstein and S. Hatjispyros and F. Vivaldi, Quasi-periodicity, global stability and scaling in a model of Hamiltonian round-off, *Chaos* **7** (1997) 49–66.

[29] J. H. Lowenstein and F. Vivaldi, Anomalous transport in a model of Hamiltonian round-off, *Nonlinearity* **11** (1998) 1321–1350.
[30] J. H. Lowenstein and F. Vivaldi, Embedding dynamics for round-off errors near a periodic orbit, *Chaos* **10** (2000) 747–755.
[31] D. A. Marcus, *Number Fields*, Springer-Verlag, New York (1977).
[32] N. Neumaerker, J. A. G. Roberts and F. Vivaldi, Distribution of periodic orbits for the Casati-Prosen map on rational lattices, *Physica D* **241** (2012) 360–371.
[33] D. Nucinkis, D. K. Arrowsmith and F. Vivaldi, Some statistical properties of discretized quasiperiodic orbits, *Nonlinearity* **10** (1997) 1643–1674.
[34] J. Pettigrew and J. A. G. Roberts and F. Vivaldi, Complexity of regular invertible p-adic motions, *Chaos* **11** (2001) 849–857.
[35] I. C. Percival and F. Vivaldi, Arithmetical properties of strongly chaotic motions, *Physica D* **25** (1987) 105–130.
[36] F. Rannou, Numerical studies of discrete plane area-preserving mappings, *Astron. Astrophys.* **31** (1974) 289–301.
[37] H. Reeve-Black and F. Vivaldi, Near-Integrable behaviour in a family of discretized rotations, *Nonlinearity* **26** (2013) 1227–1270.
[38] H. Reeve-Black and F. Vivaldi, Asymptotics in a family of linked strip maps, *Physica D* **290** (2015) 57–71. [DOI: 10.1016/j.physd.2014.09.003.] *Nonlinearity* **26** (2013) 1227–1270.
[39] R. E. Schwartz, Outer billiards and the pinwheel map, *J. Mod. Dyn.* **5** (2011) 255–283.
[40] R. E. Schwartz, Outer billiards on kites, Annals of Mathematical Studies No. 171, Princeton University Press (2009).
[41] J.-P. Serre *A Course in Arithmetic*, Springer-Verlag, New York (1973).
[42] C. Scovel, On symplectic lattice maps, *Phys. Lett. A*, **159** (1991) 396–400.
[43] J. H. Silverman, *The Arithmetic of Dynamical Systems*, Springer-Verlag, New York (2007).
[44] E. Thiran and D. Verstegen and J. Weyers, p-adic dynamics, *J. Stat. Phys.*, **54** (1989) 893–913
[45] F. Vivaldi, Periodicity and transport from round-off errors, *Experimental Mathematics* **3** (1994) 303–315.
[46] F. Vivaldi, The arithmetic of discretised rotations, in *p-adic mathematical physics* AIP Conf. Proc. **826** (2006) Amer. Inst. Phys, Melville, NY, 162–173.
[47] F. Vivaldi and I. Vladimirov, Pseudo-randomness of round-off errors in discretized linear maps on the plane, *Int. J. of Bifurcations and Chaos* **13** (2003) 3373–3393.
[48] I. Vladimirov, Discretization of dynamical systems, preprint, Deakin University, Geelong, Victoria. (1996). [I.Vladimirov@mailbox.uq.edu.au]
[49] F. Woodcock and N. P. Smart, p-adic chaos and random number generation, *Exp. Math.*, **7**, (1998) 334–342.
[50] X-S Zhang and F Vivaldi, Small pertubations of a discrete twist map, *Ann. Inst. Henry Poincaré* **68** (1998) 507–523.

SCHOOL OF MATHEMATICAL SCIENCES, QUEEN MARY, UNIVERSITY OF LONDON, LONDON E1 4NS, UK
E-mail address: f.vivaldi@maths.qmul.ac.uk
URL: http://www.maths.qmul.ac.uk/~fv